ELECTRIC FIELD CONTROLLED OPTICAL SCATTERING IN NEMATIC LIQUID CRYSTAL FILMS

by

LAWRENCE MICHAEL DeVITO

Submitted in Partial Fulfillment

of the Requirements for the

Degree of Bachelor of Science

at the

MASSACHUSETTS INSTITUTE OF TECHNOLOGY

June, 1975

Signature of Author.....
Department of Electrical Engineering and
Computer Science, 9 May 1975

Certified by.....
Thesis Supervisor

Accepted by.....
Chairperson, Departmental Committee on Theses

ABSTRACT

The control of scattering losses with external electric fields in a nematic liquid crystal thin-film waveguide is experimentally investigated. The waveguides are 12 μm MBBA (N-(p-Methoxybenzylidene)-p-butylaniline). The light source ia a 6328 °A wavelength HeNe laser. The loss is determined to be 44 $dB \cdot cm^{-1}$ with no electric field, and 23 $dB \cdot cm^{-1}$ with an electric field of 6.25×10^{6} $V \cdot m^{-1}$. The loss is also calculated as a function of electric field strength for several waveguide modes and for several molecular orientations. The experimental and calculated results are compared.

TABLE OF CONTENTS

LIST OF FIGURES

INTRODUCTION

Nematic liquid crystals (NLC) have been studied by many groups and with varied emphases. Many electro-, thermo-, and magneto-optic effects in NLC have been characterized. Being most conveniently handled in thin films, NLC are compatible with integrated optics. To this end, there is interest in applications of NLC as waveguides (1,2). Modulation (3,4) and deflection (5) in such waveguides have been reported.

Consequently, the study of optical losses in these materials has been spurred (6,7). For MBBA (N-(p-Methoxy-benzylidene)-p-butylaniline) waveguides at 6328 °A wavelength, two papers (3,5) reported losses of approximately 40 $dB \cdot cm^{-1}$, another (4) reported a loss of less than 1 $dB \cdot cm^{-1}$. This discrepancy has not yet been resolved.

Scattering in NLC is caused by long range fluctuations in the ordering of the molecular axes. In a waveguide this scattering causes coupling from guided modes to radiating modes; and energy that is radiated is considered as a loss. External electric fields applied to a waveguide have been suggested recently (7) to reduce this scattering loss. The electric fields accomplish this by reducing the fluctuations of the molecular axes' ordering.

This project is an experimental investigation of the reduction of scattering loss in a thin-film NLC waveguide, using external electric fields. The waveguides used are

12 μm films of MBBA at 6328 °A wavelendth. The substrates are glass with transparent gold electrodes. The loss is measured as 44 $dB \cdot cm^{-1}$ with no fields, and 23 $dB \cdot cm^{-1}$ with a 6.25×10^{6} $V \cdot m^{-1}$ electric field. The loss profile versus electric field strength is calculated and compared to the experimental results. The waveguides are analyzed photogrammetrically.

THEORY

Nematic liquid crystals (NLC) are cigar shaped molecules. A unit vector of arbitrary sign, parallel to the long axis of the molecule is defined as the director, $\hat{n}$. These molecules have an anisotropic dielectric susceptibility. This means that the polarizability parallel to $\hat{n}$ is different from that normal to $\hat{n}$. The molecules are also birefringent, which means that the index of refraction parallel to $\hat{n}$,(n_e) is different from that normal to $\hat{n}$,(n_o). This is illustrated schematically in Figure 1.

The large scattering loss in an NLC is caused by long range thermal fluctuations of the molecular axis ordering. Since the molecules are birefringent, fluctuations of orientation cause changes in the dielectric tensor, and strong light scattering results.

Since the NLC molecules are anisotropic at d.c., if they are subjected to a static electric field they will experience a restoring torque unless the axis of the larger susceptibility is aligned parallel to the electric field. A geometry can be selected in which the applied electric field is parallel to the induced polarization when the prefered alignment is established by other mechanisms. In this case the electric torques will reinforce the molecular alignment and reduce the thermal fluctuations in the axis ordering. The other mechanisms which impose a prefered molecular orientation include physio-chemical wall bonding (8), and inter-molecular (crystalline)

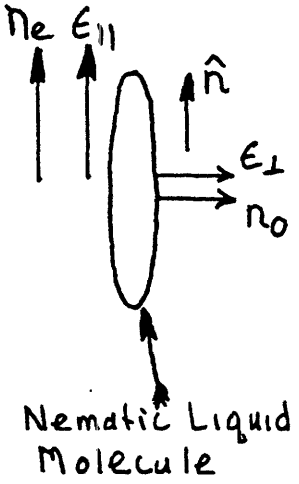

$\hat{n}$ - director

$\epsilon_{11}, \epsilon_\perp$ - parallel and perpendicular dielectric susceptibility

n_e, n_o - extra-ordinary and ordinary indices of refraction

FIGURE 1

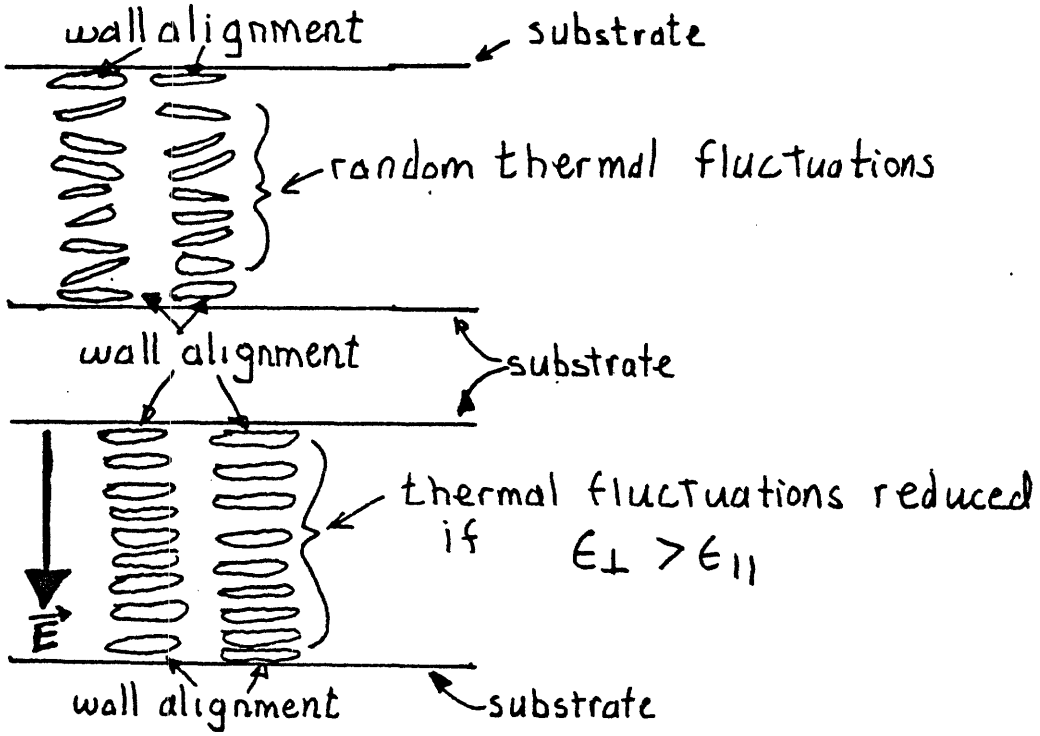

FIGURE 2

elastic forces (9). This is illustrated schematically in Figure 2. Note that in the figure the electric field is damping only one dimension of thermal vibration. The molecules are still free to vibrate in the plane normal to the page.

Waveguide Attenuation

Expressions for the loss of waveguides of NLC, taking into account an electric field, was calculated by Hu (7). The expressions derived, in units of inverse meters, are;

$$\alpha = \frac{k_B T \pi}{4 n_o^2 K} \cdot \left(\frac{\Delta \epsilon}{\lambda \epsilon_o}\right)^2 \cdot \left((2+\Delta^2) \ln \frac{1+(1+\Delta^2)^{\frac{1}{2}}}{\Delta} - (1+\Delta^2)^{\frac{1}{2}} \right) \quad \text{Eqn.(1)}$$

for TE modes, $\hat{n} \| \hat{x}$; and TM modes $\hat{n} \| \hat{y}$.

$$\alpha = \frac{k_B T \pi}{4 n_e^2 K} \cdot \left(\frac{\Delta \epsilon}{\lambda \epsilon_o}\right)^2 \cdot \left((2-\Delta^2) \ln \frac{1+(1+\Delta^2)^{\frac{1}{2}}}{\Delta} + (1+\Delta^2)^{\frac{1}{2}} \right) \quad \text{Eqn.(2)}$$

for TM modes, $\hat{n} \| \hat{x}$; and TE modes, $\hat{n} \| \hat{y}$.

$$\alpha = \frac{k_B T \pi}{4 n_o^2 K} \cdot \left(\frac{\Delta \epsilon}{\lambda \epsilon_o}\right)^2 \cdot \left(2+\Delta'^2 - \Delta'^2 (2+\frac{\Delta'^2}{2}) \ln \frac{(4+\Delta'^2)^{\frac{1}{2}}}{\Delta'} \right) \quad \text{Eqn.(3)}$$

for TE and TM modes, $\hat{n} \| \hat{z}$. Where the symbols are defined as;

$$\Delta = \left(\delta^2 + \frac{\chi_a H^2 + \epsilon_a E^2}{n_o n_e k^2 K} \right)^{\frac{1}{2}} \quad \text{Eqn.(4)} \qquad ; \delta = \frac{n_e - n_o}{n_o} \quad \text{Eqn.(5)}$$

$$\Delta' = \left(\frac{\chi_a H^2 + \epsilon_a E^2}{n_o n_e k^2 K} \right)^{\frac{1}{2}} \quad \text{Eqn.(6)}$$

$$\Delta\epsilon = (n_e^2 - n_o^2)\cdot\epsilon_o \qquad \text{Eqn.(7)}$$

$$\epsilon_a = \epsilon_{\parallel} - \epsilon_{\perp} \qquad \text{Eqn.(8)}$$

$$\chi_a = \chi_{\parallel} - \chi_{\perp} \qquad \text{Eqn.(9)}$$

k_B is Boltzman's constant

k is the wave vector of the light being scattered

n_o, n_e are the ordinary and extraordinary index of refraction of the NLC

K is the elastic constant of the NLC

The definition of the axes for these three cases is given in Figure 3. It is assumed in the figure that the electric field is properly oriented to exert restoring on the NLC molecules in each of the orientations. These fields are not shown in the figure.

Attenuation Calculations with Computer

The expressions for attenuation in waveguides were evaluated using a computer, (see Appendix III for details). The results are plotted, see Figures 4,5,and 6. The parameters used for the calculations are:

$\epsilon_a = \frac{\epsilon_o}{2}$ $\qquad$ $\chi_a = 1.5\times10^{-6}\cdot\mu_o$

$n_o = 1.521$ $\qquad$ $n_e = 1.725$

$K = 6\times10^{-12}$ Newtons

$\lambda = 6328\ ^{\circ}A = 6.328\times10^{-7}$ meter

$k = \frac{2\pi}{\lambda} = 9.929\times10^{6}$ meter^{-1}

$T = 300\ ^{\circ}K$

These calculations show that a large decrease in the loss of an NLC waveguide can be expected with the application of modest electric fields.

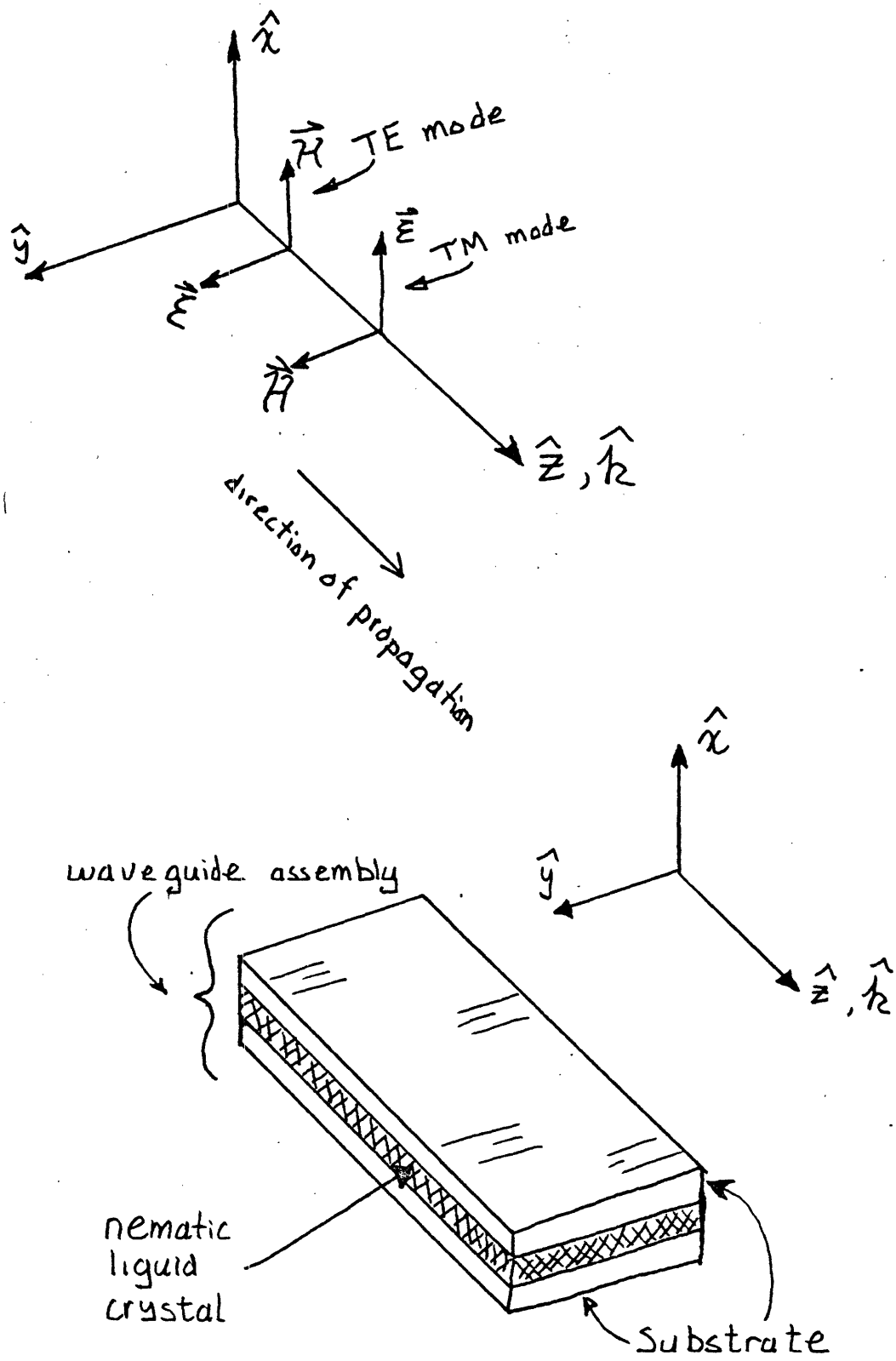
$\hat{x}$
$\vec{H}$ TE mode
$\hat{y}$
$\vec{E}$ TM mode
$\vec{E}$
$\vec{H}$
$\hat{z}, \hat{k}$
direction of propagation
$\hat{x}$
waveguide assembly
$\hat{y}$
$\hat{z}, \hat{k}$
nematic liquid crystal
Substrate

FIGURE 3

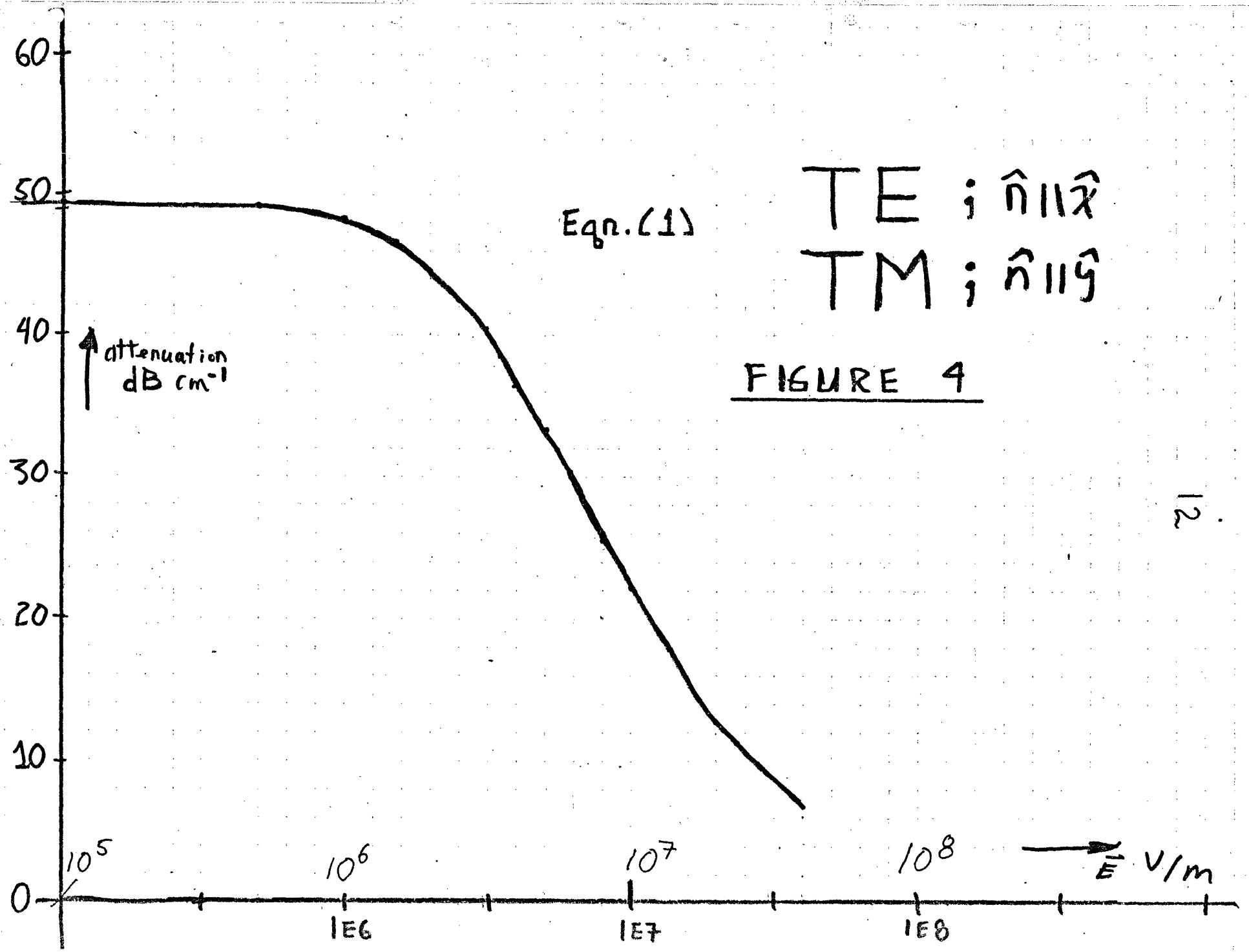

FIGURE 4

$\bar{2}$.

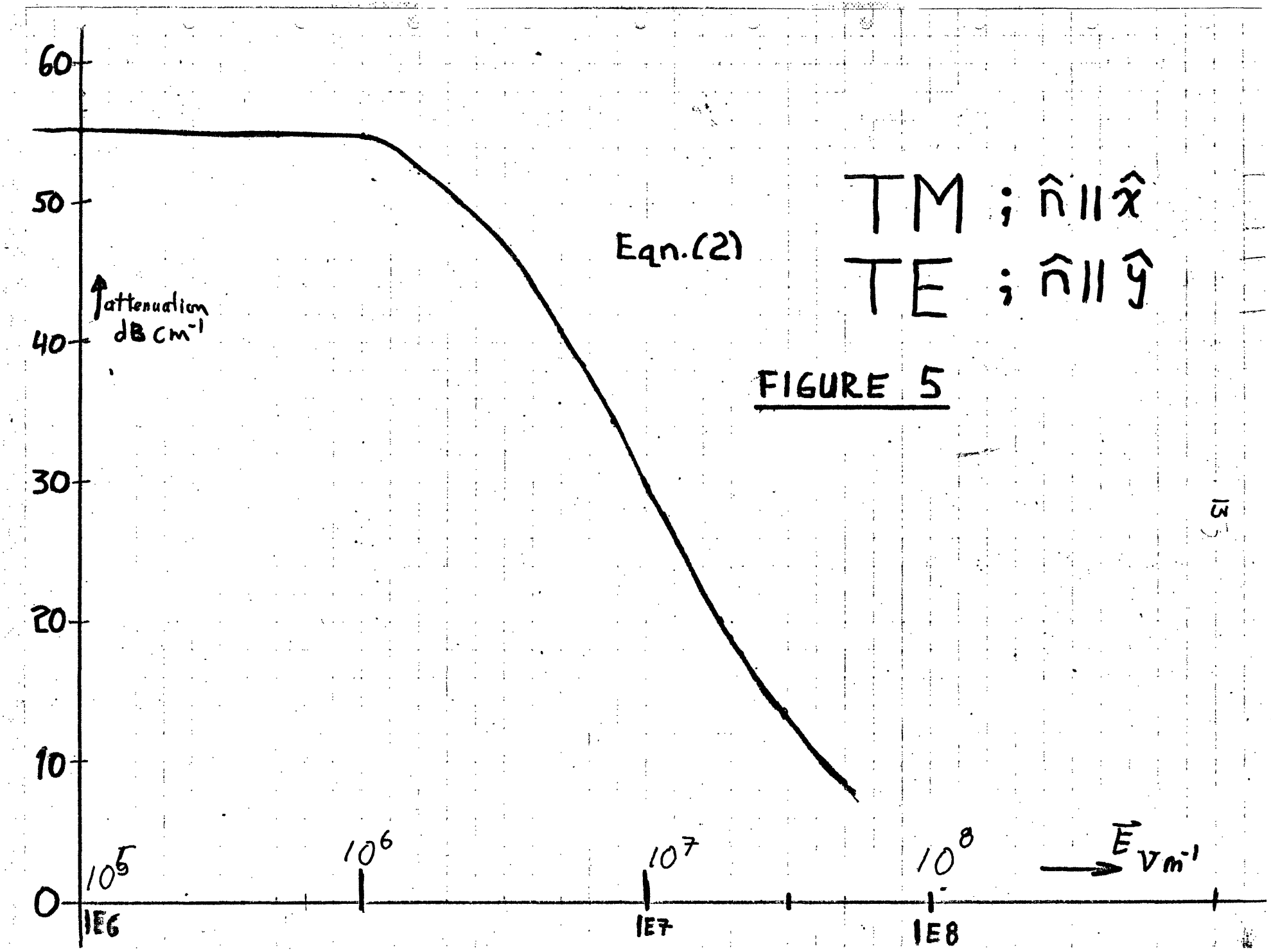
60
50
40
30
20
10
0
attenuation dB cm⁻¹
Eqn.(2)
TM ; n̂ ∥ x̂
TE ; n̂ ∥ ŷ
FIGURE 5
10⁵
10⁶
10⁷
10⁸
E V m⁻¹
1E6
1E7
1E8

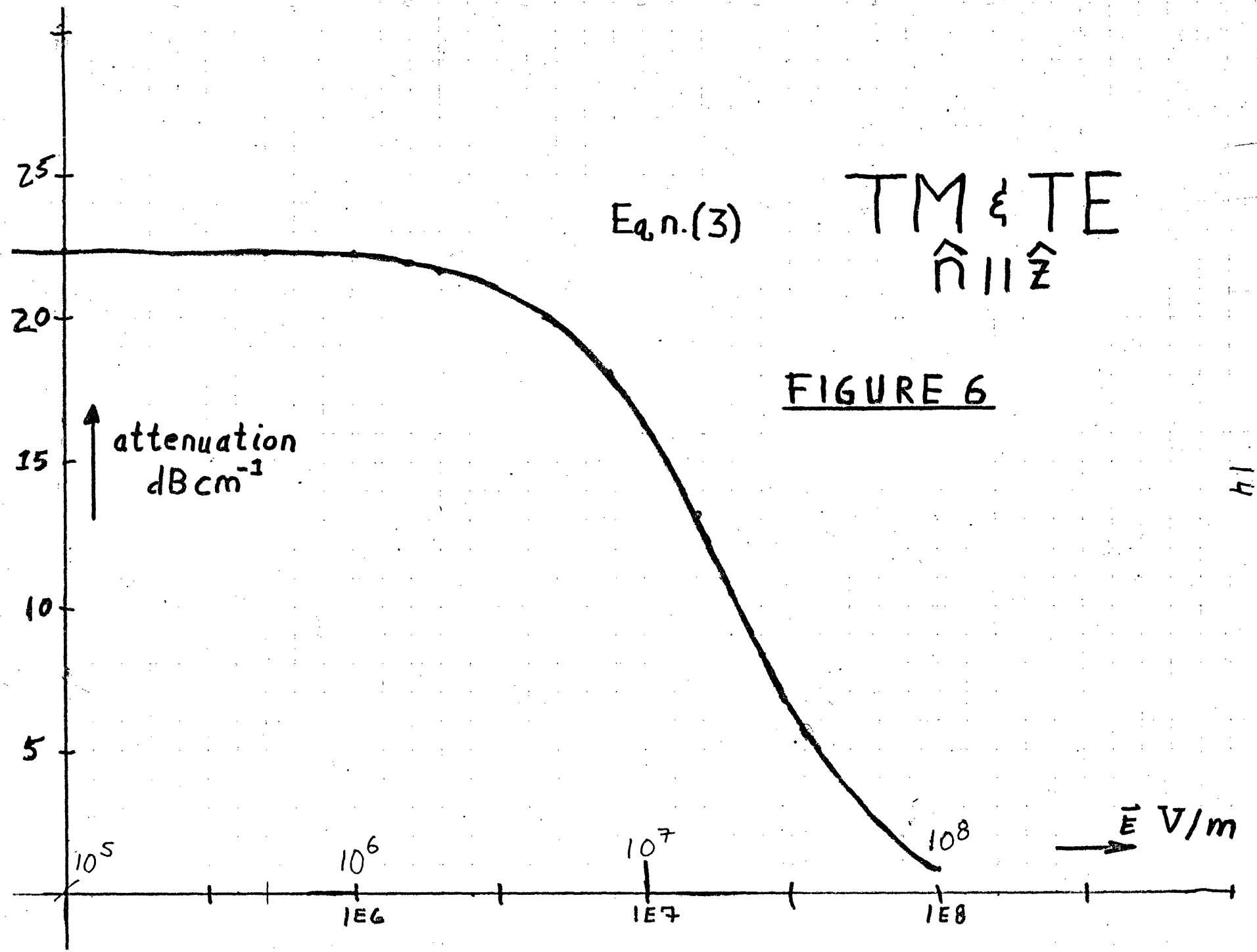
25
20
15
10
5
attenuation
dB cm⁻¹
Eqn.(3)
TM & TE
n̂ ∥ ẑ
FIGURE 6
10⁵
10⁶
10⁷
10⁸
1E6
1E7
1E8
E V/m

EXPERIMENT

The attenuation of the NLC film waveguides was measured photographically. A schematic diagram of the equipment arrangement is shown in Figure 7. A photograph of a waveguide assembly in a positioning fixture is presented in Figure 8.

The Waveguides

The waveguide assembly, shown in Figure 9, is made with glass substrates which have a transparent, conductive gold (Au) electrode on one surface. The electrode surface of each substrate is placed inward, in contact with the NLC. The dielectric spacer is a polymer film: a very commonly available polymer film is house-hold 'saran' wrap. The saran is stretched and taped to a frame, and the window is cut with a razor blade. The frame is then placed over one glass substrate, with the window centered. A drop of high purity MBBA is placed in the window and the other glass substrate is placed on top. The saran around the two substrates is then cut with a razor blade, and the whole assembly is held together with an Acco binder clip.

Special attention must be given to cleaning the substrates and the saran. Any dust or grease will cause electric arc-over and/or contaminate the NLC. The saran wash is:

1) soap and water with a camel hair brush
2) water rinse

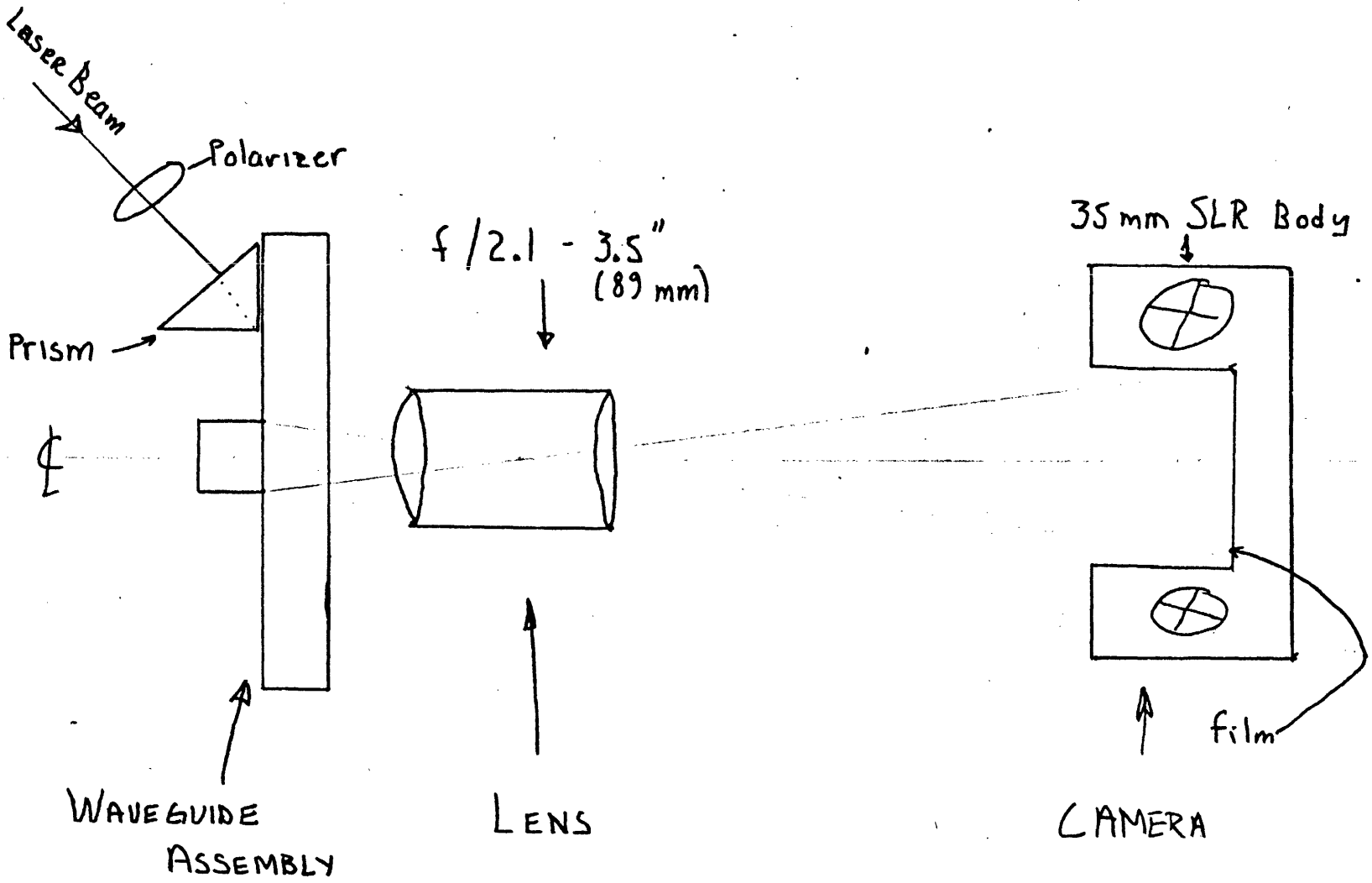
Laser Beam
Polarizer
Prism
f/2.1 - 3.5"
(89 mm)
35 mm SLR Body
Film
WAVEGUIDE
ASSEMBLY
LENS
CAMERA

FIGURE 7

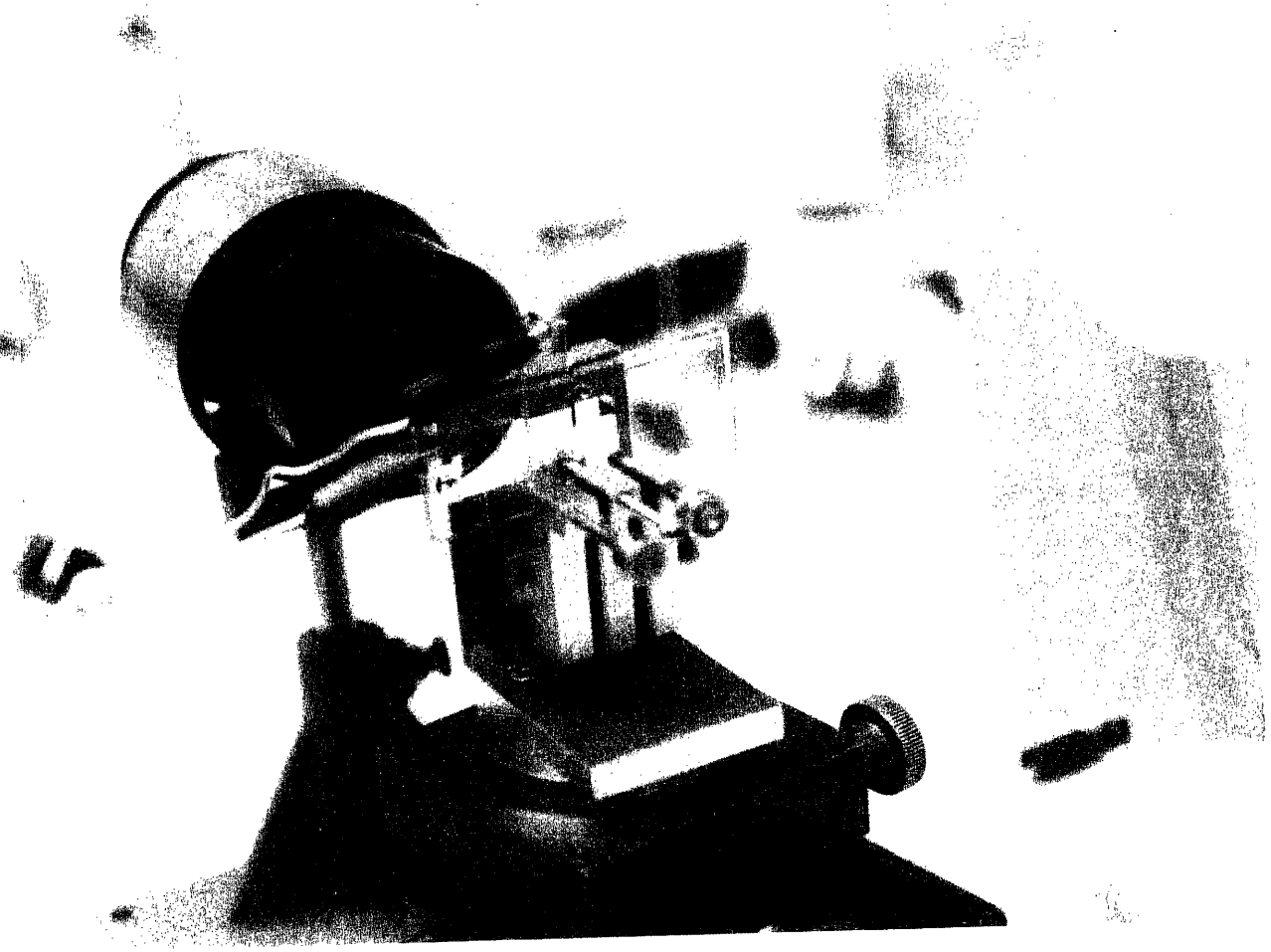

FIGURE 8

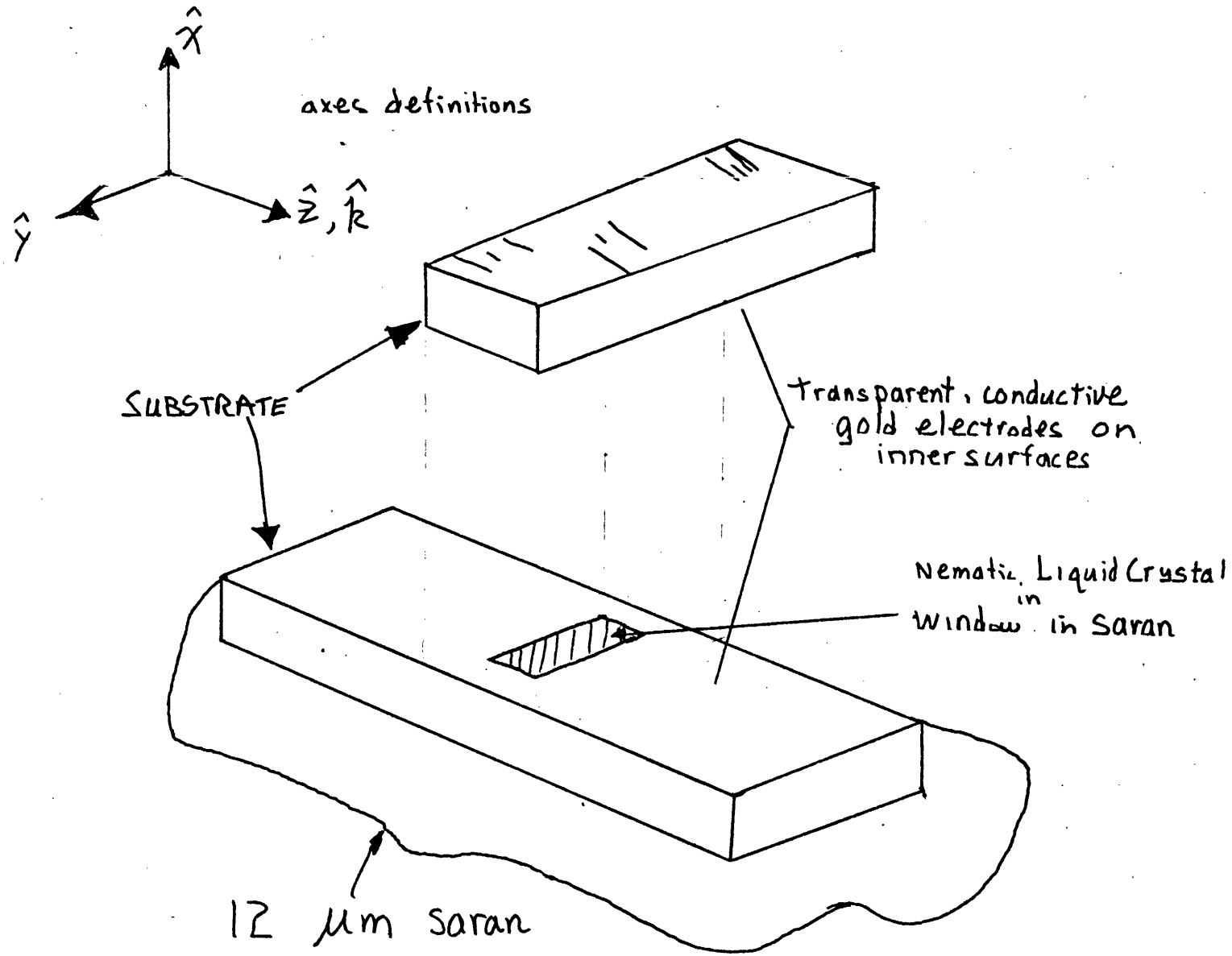
$\hat{x}$
axes definitions
$\hat{y}$
$\hat{z}, \hat{k}$
SUBSTRATE
transparent, conductive gold electrodes on inner surfaces
Nematic Liquid Crystal in Window in Saran
12 μm saran

FIGURE 9

3) acetone rinse
4) nitrogen gas blow dry

The preparation of the substrates is:

1) boil in acetone
2) soap and water with a camel hair brush
3) water rinse
4) methyl alcohol rinse
5) nitrogen gas blow dry
6) acetone rinse
7) nitrogen gas blow dry

Since the NLC being used is MBBA, which has a negative dielectric anisotropy ($\epsilon_{\parallel} > \epsilon_{\perp}$), and the electric fields are applied parallel to the $\hat{x}$ direction, an $\hat{n} \parallel \hat{y}$ surface orientation of the NLC molecules is required. The definition of the axes is given in Figure 9. To achieve an $\hat{n} \parallel \hat{y}$ orientation the slides are rubbed with a lens paper in the proper direction--parallel to $\hat{y}$.

Laser light at 6328 °A wavelength is prism coupled into the saran, and then coupled into the NLC. A bright streak in the NLC is clearly visible; it is caused by the scattering. Only the TM modes are coupled from the saran into the NLC. This is determined with a polarizer in the laser beam before the prism. When only TE modes are allowed there is no streak in the NLC; but when any TM mode is present the streak is visible. The loss measurement experiment was done <u>without</u> a polarizer , so the results are, strictly speaking, not a measure of the TM attenuation alone. However, I believe the discrepancy to be very small.

The electric field is an a.c. signal at 3 KHz. This is chosen to avoid the dynamic scattering which occurs with a d.c. field. The frequency is chosen to be faster than

the dielectric relaxation time of the NLC, again to avoid dynamic scattering.

Observations

The action of the electric field in reducing the attenuation is easily observable. Without an electric field the streak in the NLC is very bright at the incident end and decays very quickly (within about 2 mm). With an electric field, however, the streak is much longer. While it is dimmer at the incident end because of the reduction in scattering, the streak is brighter further along because of the higher intensity of the beam in the NLC at these points. These two observations are presented in Figures 10 and 11. Figure 10 is a photograph of the waveguide with no electric field applied to it. Figure 11 is the same waveguide with an electric field of 6.25×10^6 $V \cdot m^{-1}$. The waveguide is photographed with a (measured) linear magnification of 4.7 . (The prints here are a magnification of 28 diameters.) The lens is an f/number 2.1 with a focal length of 3.5 inches (89 mm). The exposure is 1 minute, with Kodak Panatomic-X film (ASA 32). Since photographic film is inherently nonlinear, some specialized data analysis techniques are necessary to interpret the photographic negatives as an attenuation in a waveguide.

No measurement was made to determine whether the scattering loss was tracking the electric field. If the response is this quick, then the measurements made here are of an

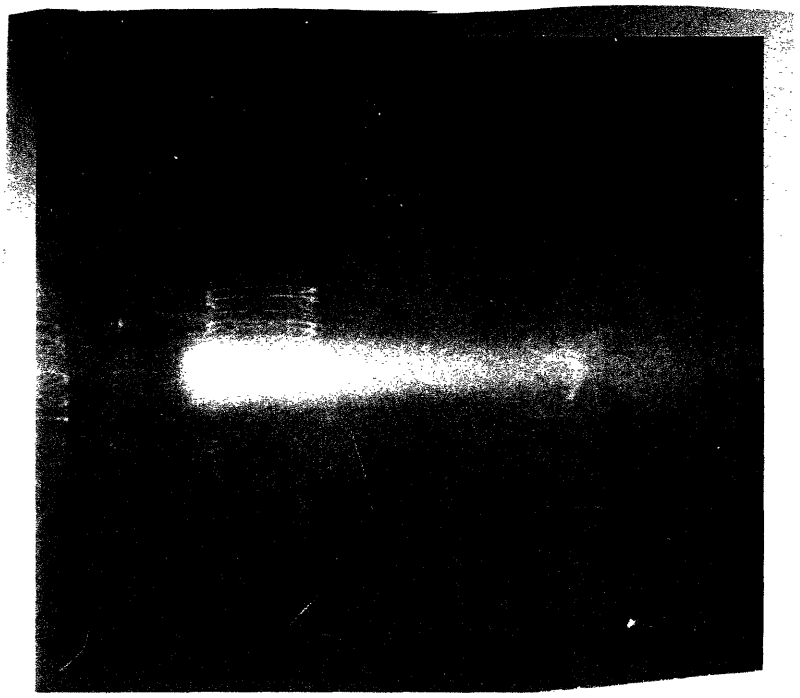

FIGURE 10

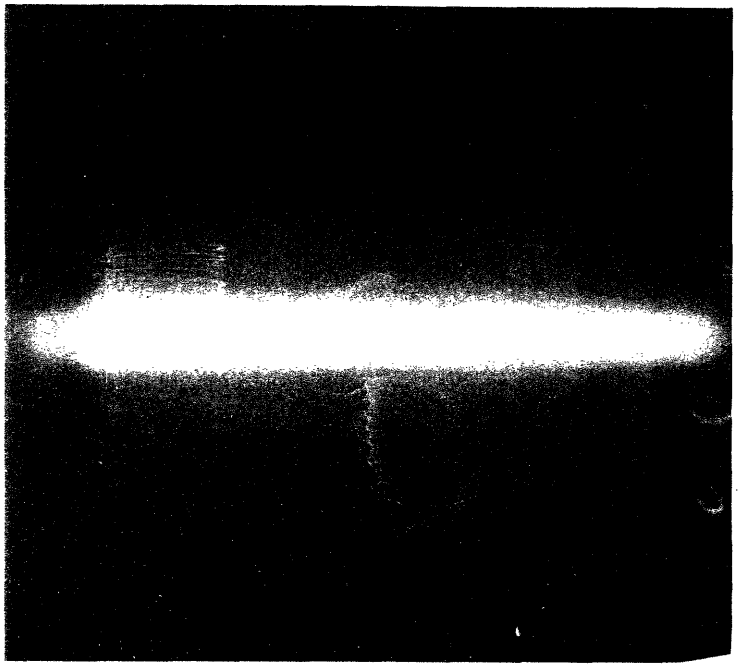

FIGURE 11

average scattering.

Photogrammetry

The nonlinearities of the photographic process complicate the analysis of the negatives. Only over a certain range of exposure does the density of the developed film vary linearly with exposure, and even then the proportionality constant, γ, is not known accurately, (10, 11). The γ is a function of many parameters, most notably the development time in the film processing. These concepts are illustrated in Figure 12.

Reciprocity Failure

There is also another factor which influences γ. The fact that 10 units of light for 1 unit of time is equivalent to 1 unit of light for 10 units of time is known as the reciprocity law (Exposure = intensity x time). However, photographic emulsions are designed to obey this law over an optimum range of light intensities and exposure times.

At very low light levels and very long exposure times, the effective γ becomes proportional to the intensity of the light. That is, the exposure is no longer the simple product of the intensity and time, rather, higher order terms become important. The γ and the contrast increase when a long exposure time is used. Since the density range of the film remains constant, a higher γ implies

D - log E TRANSFER CURVE FOR A TYPICAL PHOTOGRAPHIC EMULSION 12-A

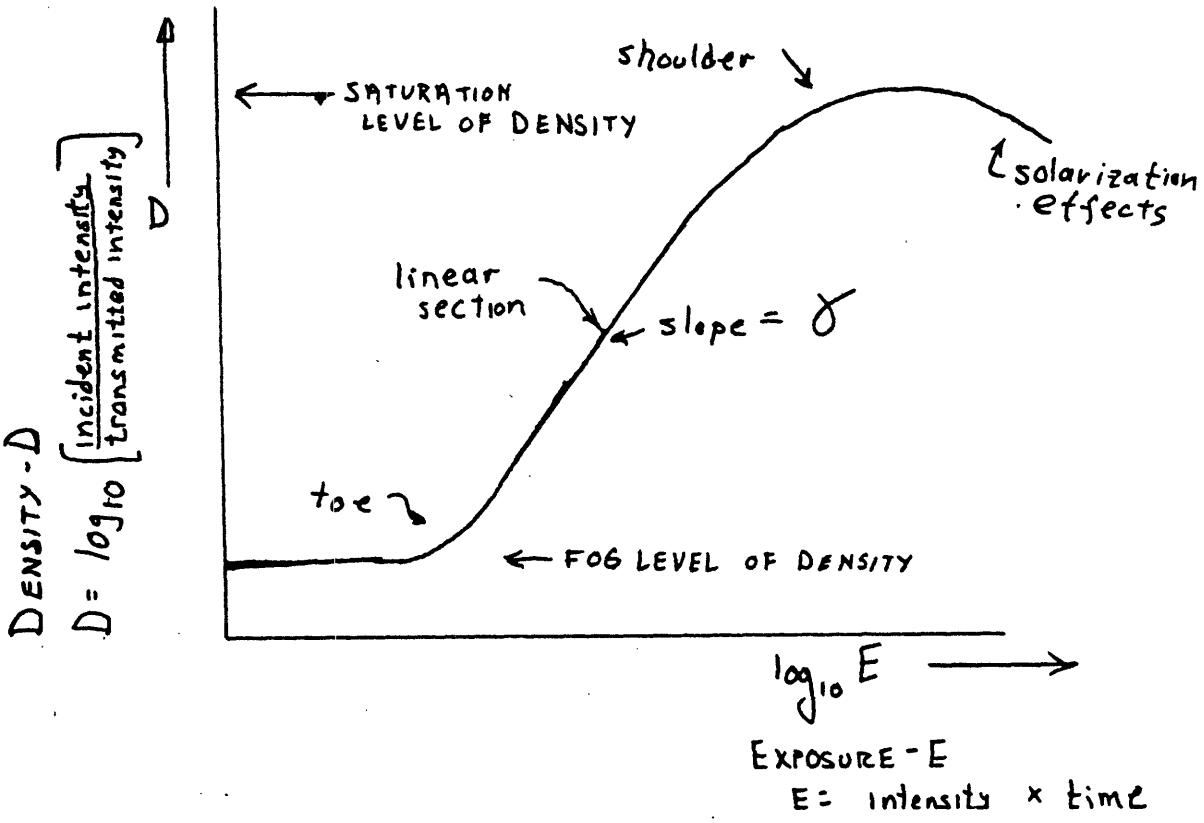

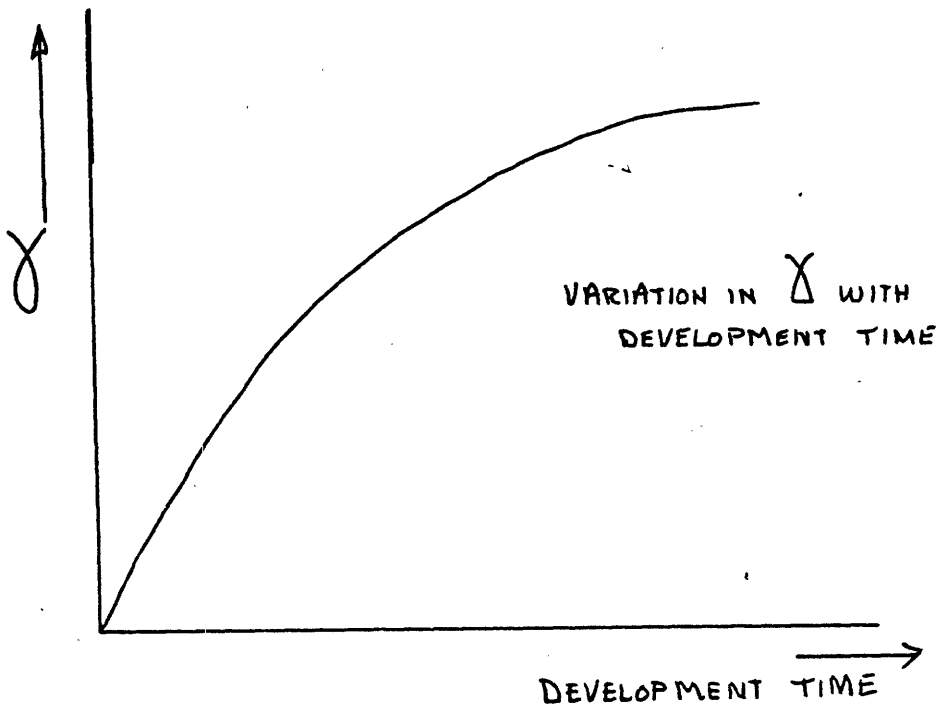

VARIATION IN γ WITH DEVELOPMENT TIME 12-B

FIGURE 12

a smaller linear range of exposure in the D-log E transfer curve. This is illustrated in Figure 13. In ordinary image photography this compensated for by simply decreasing γ with less development time in the processing of the film. However, in photogrammetry the phenomenon of reciprocity failure has more severe complicating effects.

While γ can be accurately approximated with a multiple density filter in a uniform illumination field in one exposure, or by making several exposures of different lengths of time to a uniform illumination, it is still not known in principle. Each method requires measurements at different exposures and γ is assumed constant through the measurements, and is calculated as a constant. In reality it is not constant in the range of measurement, but is a function of both intensity and exposure time.

The way out of this difficulty is to determine γ for several series of exposures, and use the average figure. One of the series is at an intensity a bit less than the object intensity being determined. Another series is at an intensity a bit more than the object intensity. And finally, a series at the same intensity level as the object intensity. The mean of the three will then accurately approximate γ of the scene being considered. Note that this method is still not adequate if a large range of intensity is to be measured in one exposure, because γ may change considerably within that range.

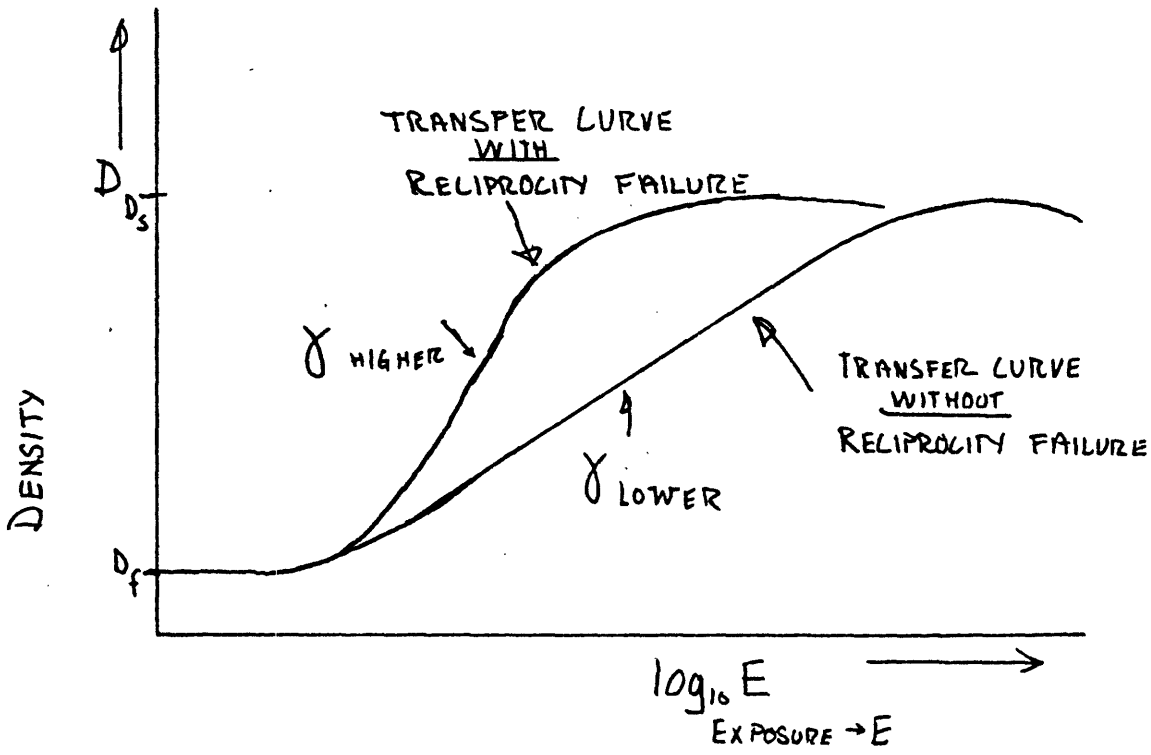

D - $\log_{10}$E TRANSFER CURVES
WITH AND WITHOUT
RECIPROCITY FAILURE

FIGURE 13

Data Analysis-γ Determination

Before the photographs of the streaks in the NLC waveguides can be analyzed, an appropriate γ must be determined. The method outlined above is used to derive the γ of the film. Five exposures were made of the waveguide; they are 1,2,3,4,and 5 minute exposures. Density measurements are taken at the same pair of points in each of the five frames. One of the points in each frame is at a low level of density. The other point (in the streak itself) is at a higher density. The γ for each series of points is computed and the average of the two is used as the γ appropriate to analyze the waveguide, since it is at an intermediate density. A microscope and an exposure meter are used to examine the small sections of each frame. The presence of reciprocity failure is clearly demonstrated since the γ measured in each case is larger than the typical γ (about 0.7) given by Kodak (10). This is because the typical γ given is for normal levels of illumination and exposure time, close to the design values of the emulsion where the reciprocity law is valid. Further, the γ for the denser series (more intense illumination) is larger than the γ for the less dense series. This confirms the reciprocity failure. The difference in density between the two series is about an order of magnitude, and the density of the waveguide to be analyzed is between the two series. The γ thus determined is 1.03 .

Waveguide Analysis

Reconstructing the exponential decay of the light scattered from the waveguides is the object of the data analysis. This is accomplished by taking samples of the density at successive points along the streak with a microdensitometer. This data is then corrected for the film nonlinearities and plotted; it should be an exponential decay. To facilitate the determination of the exponential constant, the natural logarithm of the density points is also plotted. A least squares linear regression is used to fit a straight line to these points. The slope of this line is related to the decay constant. See Appendix IV for the details of the linear regression formulae.

Microdensitometer

To sample the density of the scattering streak a microdensitometer was fashioned using a microscope (100 magnification), and a Gossen Luna Pro exposure meter. The field of view of the microscope is 1.2 mm, so the samples are therefore separated by this distance. The micrometer on the microscope stage is used to measure this increment. The Gossen exposure meter has an attachment to slide into the neck of the microscope in place of the ocular.

The Gossen is calibrated in relative f/numbers. That is, each division is a factor of two in intensity. The Relative Exposure (RE) measured at each sample point

is then given as:

$$RE = 2^{(G_n - G_1)} \qquad \text{Eqn.(10)}$$

where G_n is the Gossen reading at the n^{th} sample point, and G_1 is the reading at the reading at the first sample point. The RE is inversely proportional to the density of the film, and the density is related, through γ, to the intensity of the light scattered from the waveguide.

The expression for the transmitted light through a negative is (11):

$$T = K\, I_i^{-\gamma} \qquad \text{Eqn.(11)}$$

where I_i is the intensity incident on the film, K is a constant, and T is the transmitted intensity. Since the transmitted light is being measured relative to the first sample -- hence RE -- the constant in Eqn. (11) becomes irrelevant. The expression for the relative intensity through the film interms of the intensity incident on the film is:

$$I_i = (RE)^{-\frac{1}{\gamma}} \qquad \text{Eqn.(12)}$$

It is these data points which should follow an exponential decay. When the natural logarithm of I_i,

$$\ln I_i = \ln (RE)^{-\frac{1}{\gamma}} = -\frac{1}{\gamma} \ln (RE) \qquad \text{Eqn.(13)}$$

is plotted , it should be a straight line, whose slope is the exponential constant. Figures 14,and 15 present these plots.

Linear Regression Coefficient of Determination

Keeping in mind that the γ may not be constant over the range of brightness of the streak, the proper straight

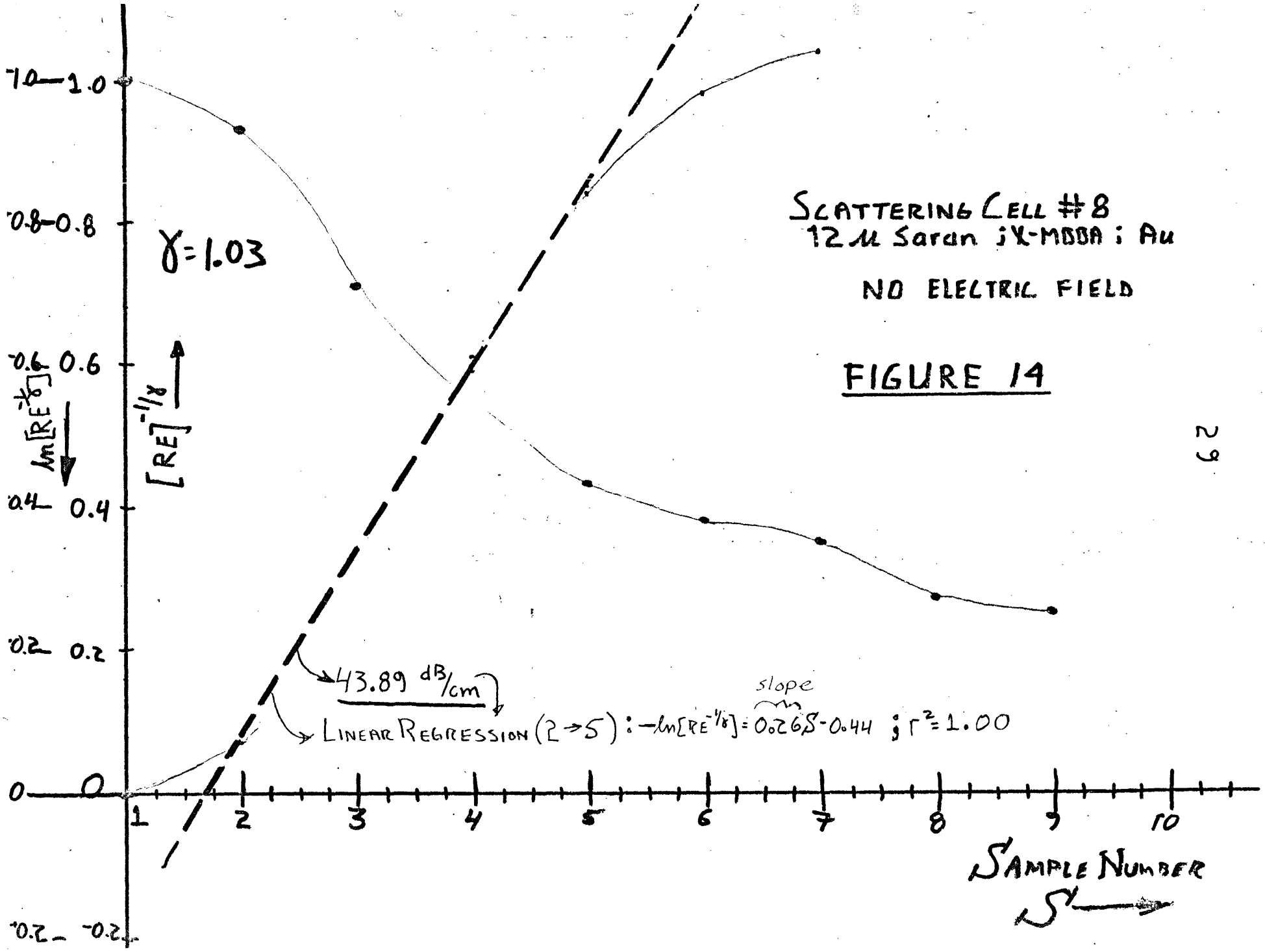

Scattering Cell #8
12 μ Saran ; X-MBBA ; Au

NO ELECTRIC FIELD

FIGURE 14

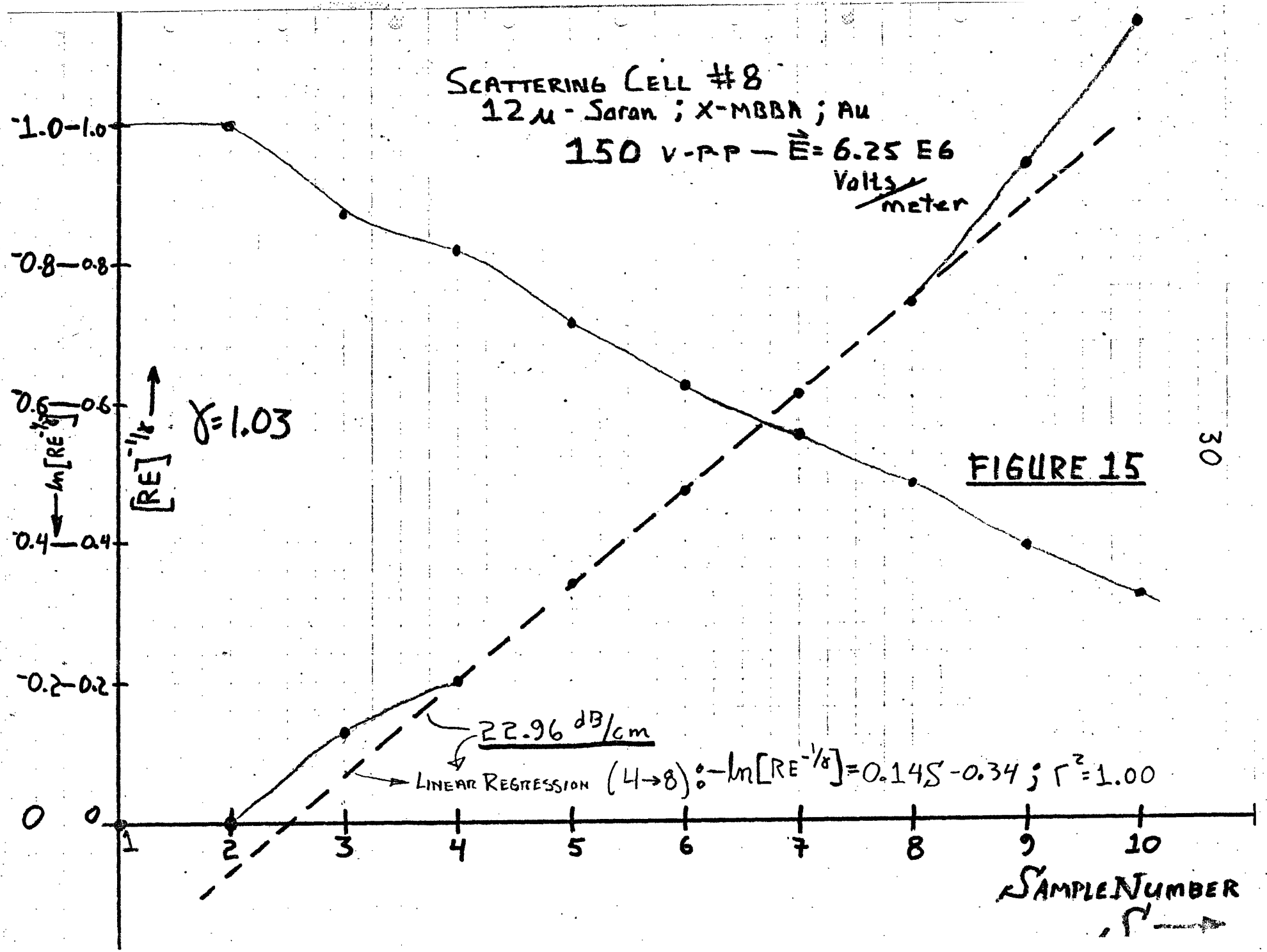
SCATTERING CELL #8
12μ - Saran ; X-MBBA ; Au
150 V-P-P — Ē = 6.25 E6 Volts/meter
-1.0
-0.8
-0.6
-0.4
-0.2
0
-ln[RE^-1/γ]
[RE]^-1/γ
γ = 1.03
22.96 dB/cm
LINEAR REGRESSION (4→8) :- -ln[RE^-1/γ] = 0.145 - 0.34 ; r² = 1.00
1
2
3
4
5
6
7
8
9
10
SAMPLE NUMBER
r
FIGURE 15

line has to be selected. This is done by taking only those contiguous samples that have the best coefficient of determination (goodness of fit parameter), r^2. See Appendix IV for details. The reasoning behind this is simple: a changing value of γ will distort the exponential curve and the 'straight line' corresponding to its logarithm will no longer be straight. By picking only those data points which fall <u>on</u> a straight line, we are assured of a constant γ for those points. Since γ is higher than normal, (because of reciprocity failure), there is a shorter linear region in the D-log E transfer curve. This means that there will only be a small section of each streak which has an intensity falling in the linear region of the film. So we expect that the data points will be colinear somewhere in the middle of the streak, and the quicker the intensity changes with distance (higher attenuation), the quicker it passes through the linear region of the film.

These effects are seen in Figures 14, and 15. In Figure 14, the zero electric field case (high loss), only four data points yielded an excellent fit ($r^2 = 1.00$). However, in Figure 15, the case with an electric field applied (low loss), five data points are colinear ($r^2 = 1.00$), indicating a slower change of intensity.

Note also that the first sample point in Figure 14, and the first three sample points in Figure 15 are at a density less than predicted by an exponential curve. This indicates that the beginning of the streak is at the saturation

density of the shoulder of the D-log E transfer curve. This means that the brightness level does indeed pass through the linear region of the film.

Relate Slope of Logarithm Plot to Attenuation

Once the slope of the line which corresponds to the natural logarithm of the exponential intensity profile is determined, it must be interpreted as an attenuation in the waveguide.

The light radiated from the waveguide is incident on the film. It is given as I_i:

$$I_i = I_o \, e^{-\alpha_f \cdot x} \qquad \text{Eqn.(14)}$$

where I_o is the intensity at the beginning of the streak, α_f is the attenuation, in units of cm^{-1}, as pictured on the film, and x is the distance from the beginning of the streak, in cm. The logarithm of this is:

$$\ln I_i = \ln I_o - \alpha_f \cdot x \qquad \text{Eqn.(15)}$$

This represents a straight line with a slope of $-\alpha_f$. It is this straight line that was determined in the previous section.

The lines were derived for axes with abscissa units of sample points, S. Each sample, S, is 0.12 cm apart, so the slope must be scaled by this factor to put it into units of cm^{-1}.

$$\alpha_f \triangleq \frac{\Delta \ln I_i}{\Delta x} = \frac{\Delta \ln I_i}{\Delta S} \cdot \frac{\Delta S}{\Delta x}$$

$$= \frac{\Delta \ln I_i}{\Delta S} \cdot \frac{1 \text{ sample}}{0.12 \text{ cm}} \qquad \text{Eqn.(16)}$$

where $\frac{\Delta \ln I_i}{\Delta S}$ is the slope of the lines in Figures 14, and 15. So the attenuation on the film then is simply given, in units of cm^{-1}, as:

$$\alpha_f = \frac{\text{slope}}{0.12} \qquad \text{Eqn.(17)}$$

Finally , we must consider the magnification of 4.7 between the waveguide and the film. The attenuation in the waveguide, α , in units of cm^{-1}, is given as:

$$\alpha = \alpha_f \cdot 4.7 \qquad \text{Eqn.(18)}$$

This can be expressed as a loss in $dB \cdot cm^{-1}$ through the following equation:

$$\text{loss } (dB \cdot cm^{-1}) = 10 \cdot \log_{10} e^{-\alpha \cdot x} \qquad \text{Eqn.(18)}$$

if x is set equal to 1 cm. The loss, in $db \cdot cm^{-1}$, in indicated in Figures 14, and 15 is calculated in this manner.

Results

The results for the $\hat{n} \parallel \hat{y}$ orientation are an attenuation of 44 $dB \cdot cm^{-1}$ with no applied field, (compared to a 49 $dB \cdot cm^{-1}$ predicted for a TM mode with $\hat{n} \parallel \hat{y}$, Figure 4). The attenuation with an electric field of 6.25×10^6 $V \cdot m^{-1}$ was 23 $dB \cdot cm^{-1}$, (compared to 28 $dB \cdot cm^{-1}$ predicted). These results are shown in Figure 16.

Note that both data points are 5 $dB \cdot cm^{-1}$ below the calculated values for a TM mode in an $\hat{n} \parallel \hat{y}$ orientation. This lower than predicted attenuation can be explained by wall alignment effects.

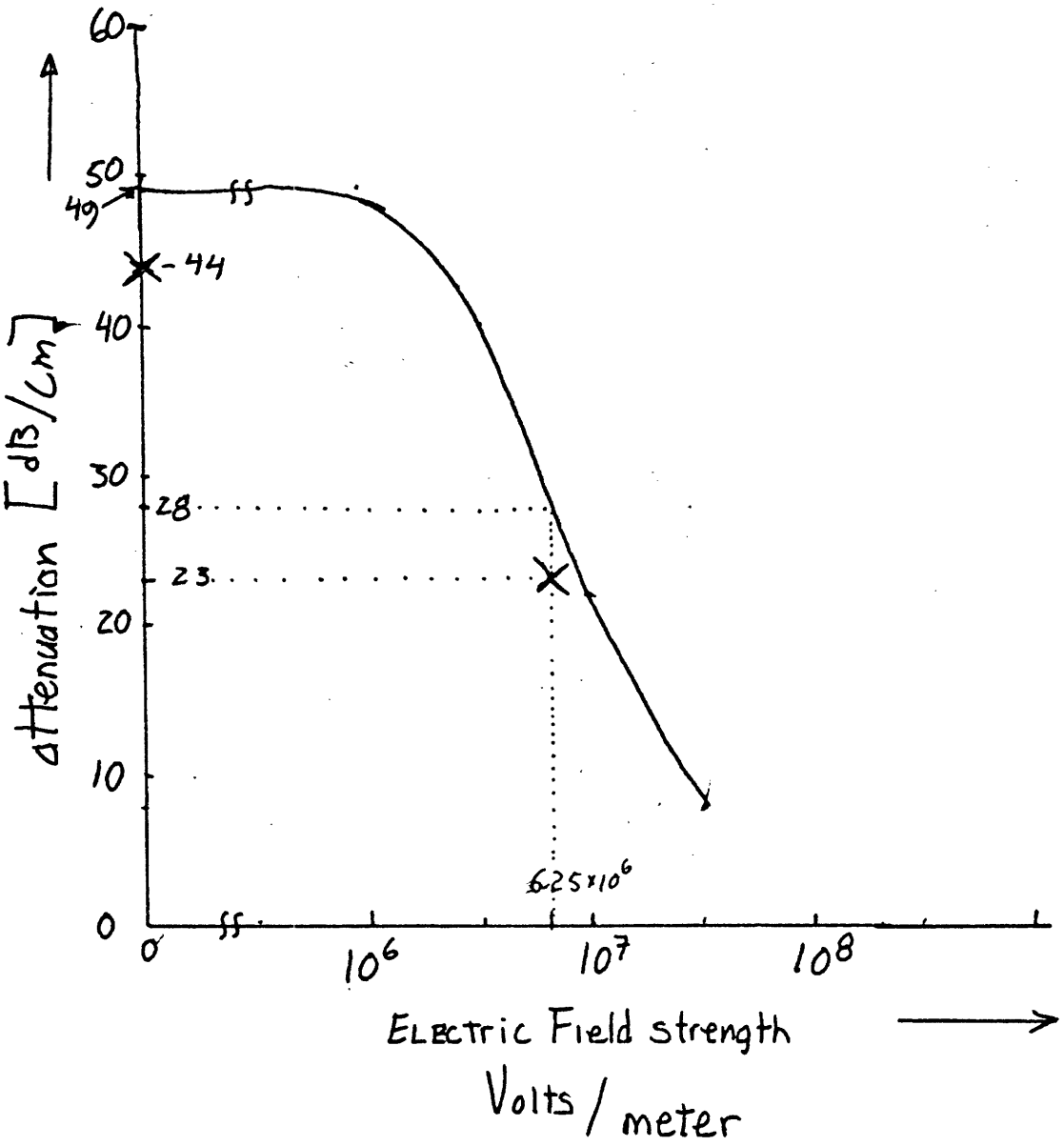
60
50
49
44
40
30
28
23
20
10
0
0
10^6
10^7
10^8
6.25×10^6
Attenuation [dB/cm]
Electric Field strength
Volts / meter

FIGURE 16

DISCUSSION

The ability to dramatically alter the attenuation in a nematic liquid crystal waveguide is demonstrated. There is a great deal of quantitative uncertainty introduced by the photographic process. However, I don't believe the ambiguity introduced exceeds 10%. Although the values of the attenuation are not known precisely, it is a safe conclusion that a 20 $dB \cdot cm^{-1}$ reduction in attenuation was demonstrated. This reduction agrees closely with that calculated.

The measured value of attenuation in the case of no electric field (44 $dB \cdot cm^{-1}$) is higher than that measured by Hu (11), (35 $dB \cdot cm^{-1}$). The higher attenuation can be caused by the thicker waveguides used here, 12 μm as opposed to 5 to 8 μm. The wall alignment effects are not as strong in the center of a thicker waveguide, hence the higher scattering. Also, the measured attenuation being 5$dB \cdot cm^{-1}$ lower than the calculated attenuation in both cases, (with and without the electric field), indicates that the wall alignment effect is indeed present.

Future work should concentrate on methods of coupling the light out of the NLC waveguide and measuring it directly. This would unambiguously determine the change in attenuation with an electric field. The absolute magnitude of the attenuation is best determined by directly measuring the scattered light at intervals along the streak. Appendix I outlines these methods.

There are many forseeable applications of this effect, amoung which are modulators, display devices, switches, and possibly shutters. Since the effect is primarily a field effect, it consumes very little power, which is an advantage over dynamic scattering devices. The bandwidth of the attenuation modulation effect was not investigated in this project. Future work should undertake this measurement.

APPENDIX I

Several other approaches to determine the attenuation in NLC waveguides were tried or considered. Most involved coupling the light out of the NLC and collecting and measuring it. This method has the advantage of eliminating all the ambiguity introduced by the nonlinearities of the photographic procedure.

Prism-in : Prism-out Coupling

This was the first method tried. It is illustrated in Figure 17. This did not work because there was no coupling from the liquid crystal into the saran, so there was no output beam to be coupled out. This probably occured because the NLC overflowed the window and extended into the area where the saran was. Because the NLC has a higher index of refraction than the saran, the light was confined to the NLC and did not couple into the saran. A possible remedy for this situation is to have the output prism in direct contact with the NLC. The disadvantage of this is the system is not sealed, and the NLC can leak out. Also, the NLC does not survive long exposures to air.

Grating-in : Grating-out Coupling

Two gratings were also tried as input and output coupling. This is illustrated in Figure 18. The gratings are Kodak Thin Film Resist (KTFR) exposed to an interference pattern

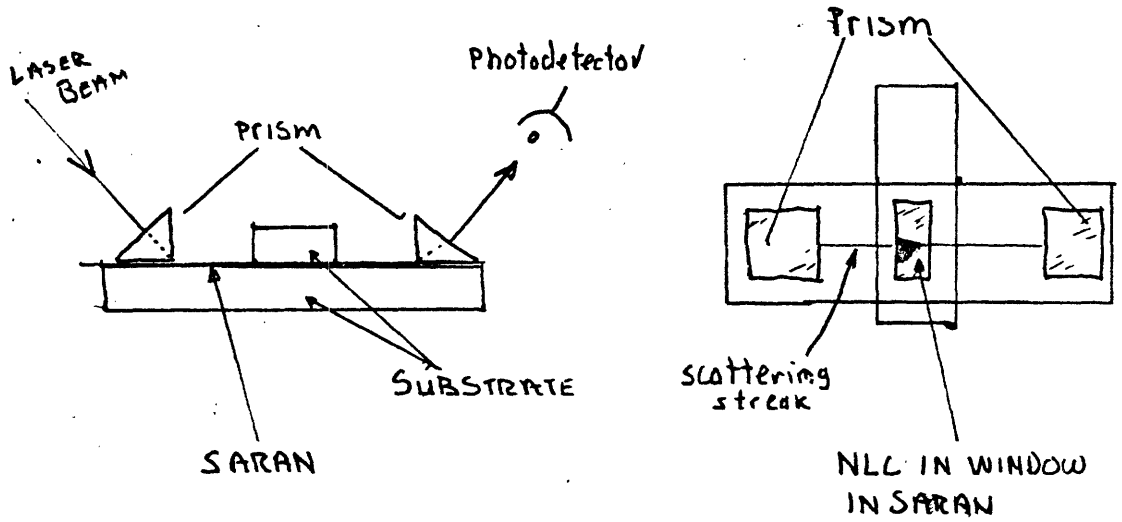

PRISM-IN : PRISM-OUT COUPLING

FIGURE 17

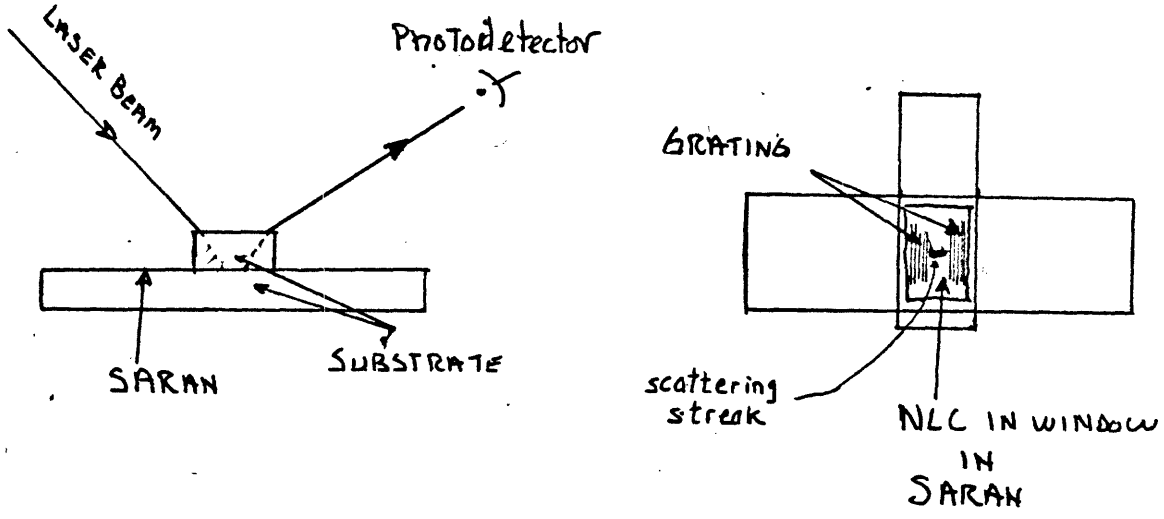

GRATING-IN : GRATING-OUT COUPLING

FIGURE 18

from two laser beams. The advantage of this method is that the use of saran is eliminated as a waveguide to carry the light from the NLC to where it can be coupled out. Rather, the NLC is in direct contact with the grating, so coupling is achieved without difficulty. The disadvantage of this method is the output beam is very difficult to detect. This is because the beams reflected from the several glass surfaces are roughly parallel to, and very much stronger than, the output beam. The output beam is weak because it has been attenuated in the NLC.

Prism-in : Grating-out Coupling

This method, using both the prism and grating coupling was not tried due to time restrictions. It is illustrated in Figure 19. This configuration has neither of the disadvantages of the two above methods. The prism coupling elimanates the multiple reflected beams that hide the true output beam. The grating output coupling provides a positive coupling of the beam from the NLC without the use of the saran. Any further work should be devoted to this method.

Television Camera

Another method, which was tried with little success, is to observe the streak in the NLC with a television camera. The measurements of the scattered light can

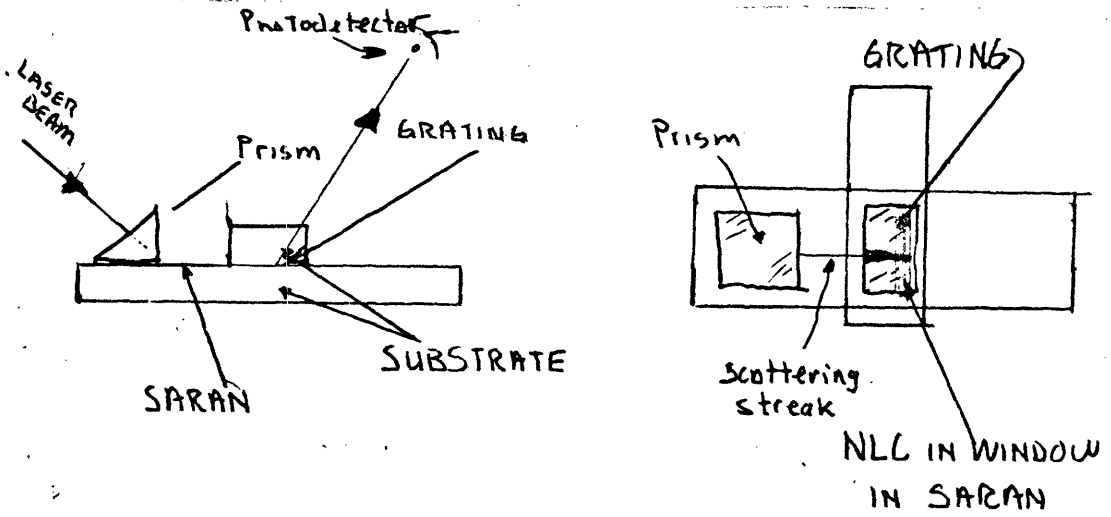

PRISM-IN : GRATING-OUT COUPLING

FIGURE 19

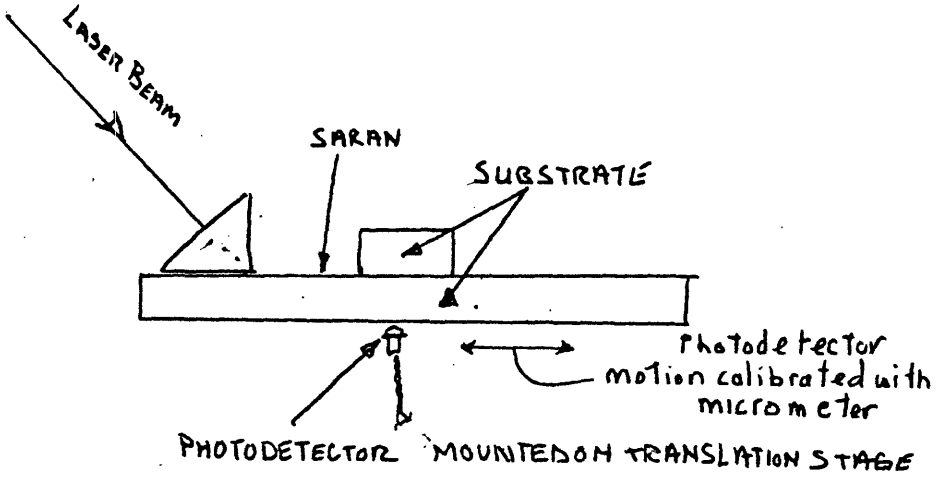

PHOTODETECTOR ON TRANSLATION STAGE

FIGURE 20

be made directly from the video signal. The advantage of this method is that a good scientific low light level television camera has a γ control. Further, γ can be measured immediately with neutral density filters. This allows an optimum selection of image intensity and camera controls to obtain a linear transfer characteristic.

This method did not work primarily because the sensitivity of the inexpensive camera used was inadequate. The signal corresponding to the streak in the waveguide was barely above the noise level. The disadvantage of this method is the expense of a good scientific low light level television camera.

Photodetector on Translation Stage

Another method, which was tried with no success at all, involves a photodetector mounted on a translation stage. The arrangement is illustrated in Figure 20. The detector is moved along the streak with a calibrated translation stage, and intensity measurements are made directly with the the photodetector. The reason this method did not work is inadequate sensitivity in the electronic instruments. Signals in the microvolt range must be measured. The disadvantage of this method is that the detector must have a very small apeture and the substrate of the waveguide must be very thin to 'see' only a small section of the streak at a time.

APPENDIX II

The NLC used in this experiment was MBBA, manufactured by Kodak. A page from a Kodak catalog (12) is reproduced here, presenting technical information on the NLC.

Nematic Materials for Electro-Optical Applications

Nematic Materials— High Resistivity, Negative Dielectric Anisotropy, Nonscattering

Eastman Organic Chemicals offers the following high-purity, high resistivity, nematic materials for use in electro-optical applications. These products are designed for those who wish to compound their own formulations or who wish to "back-dope" them with their own conductivity and aligning agents. THE PURITY OF THESE COMPOUNDS IS SUCH THAT NO DYNAMIC SCATTERING IS EXHIBITED WHEN THEY ARE EXCITED IN A TYPICAL LIQUID-CRYSTAL CELL. These products are packaged under nitrogen in septum containers.

Catalog Number

X11246

Chemical

N-(*p*-Methoxybenzylidene)-*p*-butylaniline ("MBBA")

Standard Package

5 g. $12.35

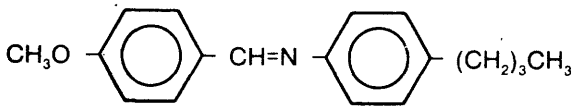

Typical Lot Data:

Nematic range: 21 to 46°C

Dielectric anisotropy (at 0.05 V_{pp}, 1.0 kHz, 25°C):

$$\varepsilon_{\perp} / \varepsilon_{\parallel} = 1.12$$

$$\varepsilon_{\parallel} - \varepsilon_{\perp} = -0.55$$

Resistivity (at 100 V_{pp}, 500 Hz, 23° C):
1×10^{11} ohm-cm

Please see notes on page 13.

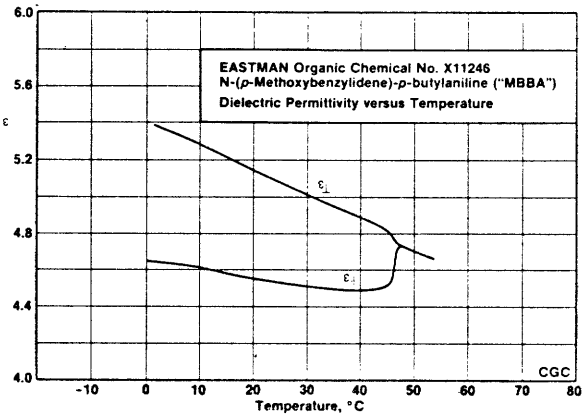

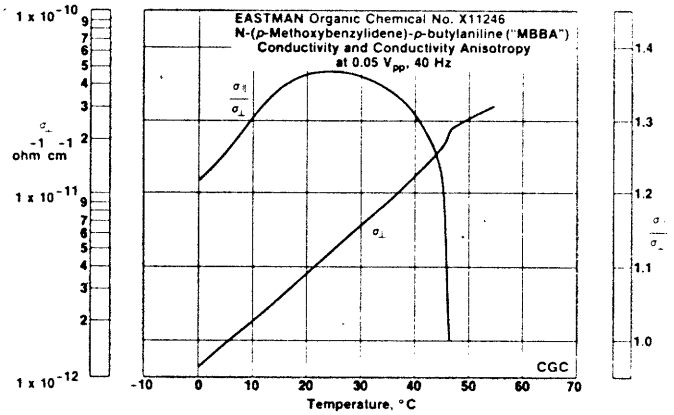

NOTES

1. The subscripts, $\perp$ (perpendicular) and $\parallel$ (parallel), refer to the relative orientation of the measuring electric field and an orienting magnetic field. Thus,
   $\varepsilon_{\perp}$ = observed permittivity (dielectric constant) for a homogenous alignment.
   $\varepsilon_{\parallel}$ = observed permittivity (dielectric constant) for a homeotropic alignment.
2. Electro-optic measurements were made on a cell with a 1/4-cm² active area and 1/2-mil spacing at 23°C.
3. For dynamic scattering materials, the optical system used a 1/4-cm² collimated light beam (λ = 632.8 nm) and had an effective *f*-number of 34.
4. For field effect materials, electro-optic measurements were made with an optical system consisting of a white-light source and a detector with an eye-response sensitivity.
5. Square-wave excitation improves contrast ratio, t_{dr} and t_r.
6. Cut-off frequency is defined as a 50% change in optical behavior.
7. Response time definitions: (See OPTICAL BEHAVIOR CURVE below)
   t_{dr} = turn-on delay t_{df} = turn-off delay
   t_r = turn-on t_f = turn-off

APPENDIX III

Computer Programs for Attenuation Calculations

The expressions for the attenuation of several modes in various molecular configurations of the waveguide are given by Eqns. (1,2,3). They were evaluated for various values of electric and magnetic fields. (The magnetic field results are not presented here.) To accomplish this several APL functions were written.

The main function is LOSS. It asks for the operating temperature and material parameters: T, K, n_e, n_o, χ_a, ϵ_a. These can be input as a constant vector, and need not be entered repeatedly. LOSS calls KNUMB, which asks for the wavelength of the light considered, and returns the wavelength and wave vector. LOSS then calls either AA1 or AA2, which calculates the constant term in the attenuation. Then, either FDEL, FDEL1, or FDEL2 is called. They each call DEL. DEL asks for the electric and magnetic field strength, and calculates Δ (DE) from them, and returns. To accomodate the difference between Δ and Δ', each of FDEL, FDEL1, and FDEL2 calculates the appropriate value of δ (D) and passes it to DEL. The difference between Δ and Δ' is that in Δ' the value of δ is zero, while in Δ its value is $\frac{n_e-n_o}{n_o}$. Each of FDEL, FDEL1, and FDEL2 then calculates the effect of the fields and passes it to LOSS. Completing the calculation, LOSS prints the attenuation in units of inverse meters. LOSS then calls DB which converts the attenuation

into units of $dB \cdot cm^{-1}$. LOSS then asks if you would like to try another value of E and H; respond YES or NO.

To calculate the different modes in different molecular configurations, LOSS is edited to call the proper functions AA1,AA2,FDEL, etc.. The appropriate functions are given below.

TE, $\hat{n} \perp \hat{x}$; TM, $\hat{n} \parallel \hat{y}$.....A = AA1 x FDEL1

TM, $\hat{n} \parallel \hat{x}$; TE, $\hat{n} \perp \hat{y}$.....A = AA2 x FDEL2

TM and TE, $\hat{n} \parallel \hat{z}$.....A = AA1 x FDEL

The APL functions are presented here.

```
      )SAVE
    22.35.44 03/14/75 CAROL
      )LIB
CAROL
      )FNS
AA1     AA2     DB      DEL     FDEL    FDEL1   FDEL2   KNUMB   L
```

```
      ∇AA1[□]∇
∇ AA1
[1]   AA←○(1.380654E¯23)×T÷4×KE×NO×NO×LAM×LAM÷((NE×NE)-NO×NO)*2
∇
```

```
      ∇AA2[□]∇
∇ AA2
[1]   AA←○(1.380654E¯23)×T÷4×KE×NE×NE×LAM×LAM÷((NE×NE)-NO×NO)*2
∇
```

```
      ∇DB[□]∇
∇ DB
[1]   DBB←10×10⍟*A÷100
[2]   'THE LOSS, IN DECIBELS PER CENTIMETER, IS:  ';DBB
[3]   ' '
∇
```

```
      ∇DEL[□]∇
∇ DEL
[1]   'ENTER ON ONE LINE:  N AND  E:'
[2]   NE←2ρ□
[3]   N←NE[1]
[4]   E←NE[2]
[5]   DE←(((D×D)+(((XA×N×N)+EA×E×E)÷NO×NE×K×K×KE)))*÷2
∇
```

```
      ∇FDEL[□]∇
∇ FDEL
[1]   D←0
[2]   DEL
[3]   DE←DE+1E¯75
[4]   F←2+(DE×DE)-DE×DE×(2+DE×DE÷2)×⍟((4+DE×DE)*÷2)÷DE
∇
```

```
      ∇FDEL1[□]∇
∇ FDEL1
[1]   D←(NE-NO)÷NO
[2]   DEL
[3]   F←((2+DE×DE)×⍟((1+(1+DE×DE)*÷2)÷DE))-(1+DE×DE)*÷2
∇
```

```
      ∇FDEL2[□]∇
∇ FDEL2
[1]   D←(NE-NO)÷NO
[2]   DEL
[3]   F←((2-DE×DE)×⍟((1+(1+DE×DE)*÷2)÷DE))+(1+DE×DE)*÷2
∇
```

```
      ∇KNUMB[□]∇
∇ KNUMB
[1]   'ENTER WAVELENGTH, IN ANGSTROMS:'
[2]   LAM←□×1E¯10
[3]   K←(○2)÷LAM
∇
```

$$\Delta \triangleq \left(\delta^2 + \frac{\chi_a H^2 + \varepsilon_a E^2}{n_o n_e k^2 K}\right)^{\frac{1}{2}}$$

$$\Delta' \triangleq \left(\frac{\chi_a H^2 + \varepsilon_a E^2}{n_o n_e k^2 K}\right)^{1/2}$$

$$\delta = \frac{n_e - n_o}{n_o}$$

```
 FDEL1   FDEL2   KNUMB   LOSS   TABLE
)
AM×LAM÷((NE×NE)-NO×NO)*2
)
AM×LAM÷((NE×NE)-NO×NO)*2
'ENTER,, IS: ';DBR
×NE×K×K×KE)))*÷2
)
(4+DE×DE)*÷2)÷DR
DE))-(1+DE×DE)*÷2
)
DE))+(1+DE×DE)*÷2
)
```

```
      ∇LOSS[⎕]∇
∇ LOSS
[1]   'ENTER ON ONE LINE:  T,      KE,      NE,      NO,
[2]   V←6⍴⎕                                    XA,  EA
[3]   T←V[1]
[4]   KE←V[2]
[5]   NE←V[3]
[6]   NO←V[4]
[7]   XA←V[5]×04E¯7
[8]   EA←V[6]×8.85E¯12
[9]   KNUMB
[10]  AA1
[11]  ' '
[12]  ' '
[13]  CALC:FDEL
[14]  A←AA×F
[15]  'THE LOSS, IN UNITS OF INVERSE METERS, IS:  ';A
[16]  DR
[17]  ' '
[18]  ' '
[19]  'CHANGE H OR E ?'
[20]  ANSWER←⎕
[21]  →CALC×((⍴ANSWER)=3)
[22]  →
∇
```

$$\Delta \triangleq \left(\delta^2 + \frac{\chi_a H^2 + \epsilon_a E^2}{n_o n_e k^2 K}\right)^{\frac{1}{2}}$$

$$\Delta' \triangleq \left(\frac{\chi_a H^2 + \epsilon_a E^2}{n_o n_e k^2 K}\right)^{1/2}$$

$$\delta = \frac{n_e - n_o}{n_o}$$

TE, n ∥ x ; TM, n ∥ y

$$\alpha = \frac{k_B T_H}{4 n_o^2 K}\left(\frac{\Delta\epsilon}{\lambda \epsilon_0}\right)^2 \times \left((2+\Delta^2)\ln\left[\frac{1+(1+\Delta^2)^{\frac{1}{2}}}{\Delta}\right] - (1+\Delta^2)^{\frac{1}{2}}\right)$$

$$A = AA1 \times FDEL1$$

$$\Delta\epsilon = (n_o^2 - n_e^2)\,\epsilon_0$$

TM, n ∥ x ; TE, n ∥ y

$$\alpha = \frac{k_B T_H}{4 n_e^2 K}\left(\frac{\Delta\epsilon}{\lambda \epsilon_0}\right)^2 \times \left((2-\Delta^2)\ln\left[\frac{1+(1+\Delta^2)^{\frac{1}{2}}}{\Delta}\right] + (1+\Delta^2)^{\frac{1}{2}}\right)$$

$$A = AA2 \times FDEL2$$

TM & TE, n ∥ z

$$\alpha = \frac{k_B T_H}{4 n_o^2 K}\left(\frac{\Delta\epsilon}{\lambda \epsilon_0}\right)\left(2 + \Delta'^2 - \Delta'^2\left(2 + \frac{\Delta'^2}{2}\right)\ln\left[\frac{(4+\Delta'^2)^{\frac{1}{2}}}{\Delta'}\right]\right)$$

$$A = AA1 \times FDEL$$

APPENDIX IV

Linear Regression Formulae

The linear regression analysis of the logarithm functions was done with an Hewlett Packard model HP-55 calculator. The expressions that machine uses for the linear parameters are given here:

$$y = mx + b$$

$$m = \frac{n\Sigma xy - \Sigma x \Sigma y}{n\Sigma x^2 - (\Sigma x)^2}$$

$$b = \frac{\Sigma y \Sigma x^2 - \Sigma x \Sigma xy}{n\Sigma x^2 - (\Sigma x)^2}$$

The coefficient of determination establishes how well the data fits the linear regression. It is given as:

$$r^2 = \frac{(\Sigma(x - \bar{x})(y - \bar{y}))^2}{(\Sigma(x - \bar{x})^2)(\Sigma(y - \bar{y})^2)}$$

or, equivalently,

$$r^2 = \frac{n\Sigma xy - \Sigma x \Sigma y}{n(n-1)s_x s_y}$$

where s_x and s_y are the standard deviations of the x and y data values. This equivalent foumula is given by Hewlett Packard as the most computationally efficient expression for r^2.

REFERENCES

1. T.P. Sosnowski, Opt. Commun. 4, 408 (1972)

2 C. Hu, and J.R. Whinnery, IEEE J. Quantum Electron. 10, 556 (1974)

3 D.J. Channin, Appl. Phys. Lett. 21, 365 (1973)

4 J.P. Sheridan, J.M. Schmur, and T.G. Giallorenzi, Appl. Phys. Lett. 22, 560 (1973)

5 C. Hu, J.R. Whinnery, and N.M. Amer, IEEE J. Quantum Electron. 10, 218 (1974)

6 P.G. DeGennes, Mol. Cryst. Liq. Cryst., 7, 325 (1969)

7 C. Hu, and J.R. Whinnery, J. Opt. Soc. Am. vol. 64; no.11, 1424 (1974)

8 F.J. Kahn, G.N. Taylor, and H. Schonhorn, Proc. IEEE 61, 823 (1973)

9 F.C. Frank, Discuss. Faraday Soc., vol. 25, p.19 (1958)

10 Kodak Publication No. F-5; Kodak Professional Black and White Films, First Edition, (1969), (1971) Eastman Kodak Co., Rochester, NY 14650

11 A.R. Schulman, Principles of Optical Data Processing for Engineers, N.A.S.A. Technical Report No. R-327, National Technical Information Service, Publication No. N70-33778, Springfield, VA 22151

12 Kodak Publication No. JJ-14; Eastman Liquid Crystal Products, (1972). Eastman Kodak Co., Rochester, NY 14650